



Measurement of $Z/\gamma^* + \text{jet} + X$ angular distributions in $p\bar{p}$ collisions at $\sqrt{s} = 1.96$ TeV

The DØ Collaboration
URL <http://www-d0.fnal.gov>
(Dated: March 17, 2009)

We present the first measurements of $\Delta\phi_{Z,\text{jet}}$, $\Delta y_{Z,\text{jet}}$ and $y_{\text{boost}}(Z + \text{jet})$ in $Z/\gamma^* + \text{jet} + X$ events at a hadron collider. Vector boson production in association with jets is an excellent probe of QCD, and constitutes the main background to many small cross section processes, such as associated Higgs production. These measurements are crucial tests of the predictions of perturbative QCD and current event generators, which have varied success in describing the data. Using these measurements as inputs in tuning event generators will increase the experimental sensitivity to rare signals.

Preliminary Result for Winter 2009 Conferences

I. INTRODUCTION

The production of the massive vector bosons W and Z/γ^* at hadron colliders, such as the Fermilab Tevatron and CERN Large Hadron Collider, is interesting for a number of reasons. The electron and muon decay modes of these bosons are experimentally rather simple to identify in such complex physics environments, and they can be used as a non-colour-connected probe of the hadron collision. Vector boson production in association with jets (V+jets) generally lies within the regime of perturbative QCD (pQCD). However such complex final states are difficult to calculate to higher orders in perturbative theory. V+jets is also the experimental signature of many other processes with significantly smaller cross sections, such as top pair production, associated production of the Higgs boson, and the decays of particles within many super-symmetric scenarios. A precise understanding of V+jets is therefore key to separating and identifying such rare processes under the V+jets backgrounds.

This note describes the first measurement at a hadron collider of the Z/γ^* +jet+X production cross section, differential in the angles between the Z/γ^* and jet. Previous measurements at the Tevatron have included the Z/γ^* transverse momentum distribution (p_T^Z) and rapidity (y^Z) [1–3]; the Z/γ^* cross section in bins of jet multiplicity [4]; the leading jet p_T and rapidity in Z/γ^* production, as well as p_T^Z and y^Z in events with at least one jet [5]; and the p_T of the leading, second and third jet associated with Z/γ^* production [6, 7]; as well as studies of W and Z/γ^* production in association with heavy flavors [8–11].

This analysis uses a dataset of $p\bar{p}$ collisions corresponding to an integrated luminosity of $0.97 \pm 0.06 \text{ fb}^{-1}$ [12] recorded by the D0 detector between April 2002 and February 2006. The measurement is carried out using the $Z/\gamma^* \rightarrow \mu^+\mu^-$ decay mode, in a di-muon mass region (65–115 GeV) in which the Z/γ^* production cross section is almost exactly the same as for pure Z production. Differential cross sections are measured, binned in the azimuthal angle between the Z/γ^* and leading jet, $\Delta\phi_{Z,\text{jet}}$; the rapidity difference between the Z/γ^* and leading jet, $\Delta y_{Z,\text{jet}}$; and the average rapidity of the Z/γ^* and leading jet, $y_{boost}(Z + \text{jet})$. These measurements are made with selection criteria which optimize the detector acceptance and resolution, and reveal the main differences between theoretical predictions: $p_T^{\text{jet}} > 20 \text{ GeV}$, $|y^{\text{jet}}| < 2.8$, $|y^\mu| < 1.7$, and for two p_T^Z ranges: $p_T^Z > 25 \text{ GeV}$, and $p_T^Z > 45 \text{ GeV}$.

Comparisons to the data are made using pQCD predictions from MCFM [13], with suitable non-perturbative corrections applied. Several tools have been developed for generating full V+jets events, starting with the parton-shower event generators PYTHIA [14] and HERWIG [15], and tools to combine tree level matrix element calculations with parton showers, such as SHERPA [16] and ALPGEN [17], which uses with PYTHIA or HERWIG for showering and hadronisation. Comparisons between these generators show differences in the predicted kinematics of V+jet production [18], so inputs from measurements are needed to improve these models. Predictions from these models are compared to the data in the distributions measured here.

II. SELECTION

A full description of the D0 detector is available elsewhere [19], and only the most relevant components are described here. Immediately surrounding the $p\bar{p}$ interaction region are two tracking detectors: a silicon microvertexing tracker, and a scintillating fiber tracker, housed inside a solenoidal magnet providing a field of 2 T. These trackers are used to measure the momenta of charged particles, and to reconstruct the primary interaction point in each collision. Outside the solenoid magnet lies a liquid argon and uranium calorimeter, which is split into three sections: a central section extending to $|\eta| < 1.1$ [20]; and two forward sections covering $1.4 < |\eta| < 4$. Scintillating material provides additional measurements between the central and forward calorimeters. Outside the calorimeter lie three layers of muon detectors, which are a combination of scintillating pixels and drift tubes. Between the first and second layer lies a 1.8 T toroidal magnet, allowing an independent momentum measurement.

Events used in this analysis are selected by least one of a suite of single muon triggers. Each of these triggers uses fast readout from the muon system scintillators and fibre tracker to initially identify events, then information from the full tracking and muon systems to provide further rejection. Further selections are then applied to obtain a pure sample of Z/γ^* + jets. Two muons of opposite charge and $p_T > 15 \text{ GeV}$ are required, using information from the muon detectors and the tracking system. The reconstructed di-muon mass is required to be in the range $65 < M_{\mu\mu} < 115 \text{ GeV}$. To reject cosmic rays and poorly reconstructed muons, the associated tracks are required to match the reconstructed primary interaction point both transverse and parallel to the beam direction; the two muon tracks are also required not to be collinear. Finally, the muons are required to be consistent with the $p\bar{p}$ bunch crossing time, using information from the muon system scintillators.

Jets are reconstructed using the D0 Run II seeded, iterative mid-point cone algorithm [21] on clusters of energy deposited in the calorimeter. The algorithm is configured with a split-merge fraction of 0.5 and cone size of $\Delta\mathcal{R} = \sqrt{(\Delta\phi)^2 + (\Delta y)^2} = 0.5$, where y is the rapidity [22]. Shape and quality cuts reject jets caused by noise in the calorimeter. Further corrections are applied for the calorimeter response; instrumental out-of-cone showering effects;

and additional energy deposits caused by instrumental noise and pile-up from multiple interactions and previous $p\bar{p}$ bunch crossings. These corrections are derived by balancing the p_T in $\gamma + \text{jet}$ events, where the γ and jet are opposite in ϕ . After corrections, jets are required to have $p_T > 20$ GeV.

Further selections are applied to limit the measurement to regions with high detection efficiency and well understood detector performance: the muons are required to have $|\eta| < 1.7$, the primary vertex to lie within 50 cm of the centre of the detector along the direction of the beam; and jets are required to have $|y| < 2.8$. After these selections, the highest p_T jet is selected to calculate the angular variables.

The main source of background in this analysis is muons from semi-leptonic decays in high energy jets or $W + \text{jet}$ production. This is reduced to negligible levels ($< 0.5\%$ of the final sample) by limiting the sum of track momenta and the calorimeter energy allowed around each muon. The muons are also required to not overlap with any jet by requiring angular separation $\sqrt{(\Delta\phi(\mu, \text{jet}))^2 + (\Delta\eta(\mu, \text{jet}))^2} > 0.5$. Other sources of background (e.g., top quark production, $Z/\gamma^* \rightarrow \tau^+\tau^-$) are estimated using simulation and found to be negligible ($< 0.1\%$). A total of 59,336 $Z/\gamma^* \rightarrow \mu^+\mu^-$ candidate events are selected before jet requirements, of which 9,927 contain at least one jet passing all selections.

III. EVENT SIMULATION AND ANALYSIS METHOD

To extract differential cross sections, the measured $Z/\gamma^* + \text{jet} + \text{X}$ events must be corrected to the particle level [23], by correcting for detector resolution, acceptance and efficiency. These corrections are derived from simulated $Z/\gamma^* + \text{jet} + \text{X}$ events. Events are generated with ALPGEN v2.11, CTEQ6L1 PDF [24], and showered using PYTHIA v6.413 with the ‘‘Tune-A’’ underlying event settings [25]. These simulated events are then passed to a GEANT [26] based full detector simulation, and real data events from random bunch crossings are overlaid on the simulation to reproduce the effects of multiple $p\bar{p}$ interactions and detector noise.

In order to accurately describe the data, and hence detector to particle level correction factors, further adjustments must be made to the simulation. The muon trigger is not simulated; instead the trigger efficiency is measured in data, and parameterised in terms of the geometry of the muon system. This efficiency is then applied on an event-by-event basis to the simulation, with the average efficiency being $(88.3 \pm 0.3)\%$, quoting just the statistical uncertainty. The efficiency of the muon reconstruction and isolation requirements are measured in data and in simulations, and small scale factors are applied to simulation to correct for any differences. The muon p_T resolution is studied by comparing the shape of the Z/γ^* mass peak in data and simulation, and further smearing is applied to simulation to reproduce the data. Jets are studied by measuring the p_T balance in back-to-back $Z/\gamma^* + \text{jet}$ configurations, and further scaling and smearing is applied to the simulation to match data. Finally, kinematic variables are re-weighted in the simulation to provide a good simultaneous description of the variables important to this analysis: p_T^Z , p_T^{jet} , y^{jet} , as well as $\Delta\phi_{Z,\text{jet}}$, $\Delta y_{Z,\text{jet}}$ and $y_{\text{boost}}(Z + \text{jet})$. After these corrections, the simulation provides a good description of the measured distributions.

The distributions of $\Delta\phi_{Z,\text{jet}}$, $\Delta y_{Z,\text{jet}}$ and $y_{\text{boost}}(Z + \text{jet})$ are binned, with the binning determined by a combination of detector resolution, maintaining reasonable statistics in each bin, and maximizing sensitivity to shape differences predicted by different models of $Z/\gamma^* + \text{jet}$ production. A statistical uncertainty is assigned to each bin, equal to the square root of the number of measured events in that bin. The ratio of particle level to detector level quantities in the simulation is then calculated, then applied to the detector level data to correct back to the particle level. The data are then normalised to the total Z/γ^* production cross section measured with this sample, which leads to a cancellation of many uncertainties.

Finally, systematics are assessed. Several sources of systematic uncertainty are considered, mainly coming from the adjustments applied to simulation to match data: muon p_T resolution, jet p_T resolution, energy scale and efficiency. These corrections are shifted individually up then down one standard deviation, and the detector to particle level corrections re-derived. The difference in the final result is assigned as a systematic uncertainty. The effects of the various kinematic re-weightings is assessed by turning each of these off in turn, and repeating the analysis; however, it is found that the result is largely insensitive to these tests. The systematic uncertainties are combined in quadrature, and for the selection with $p_T^Z > 25$ GeV the total is of comparable size to the statistical uncertainty; for the selection with $p_T^Z > 45$ GeV, the statistical uncertainty dominates.

IV. RESULTS

The following normalised differential cross sections have been measured:

- $1/\sigma_{Z/\gamma^*} \times d\sigma_{Z/\gamma^*+jet}/d\Delta y_{Z,jet}$
- $1/\sigma_{Z/\gamma^*} \times d\sigma_{Z/\gamma^*+jet}/dy_{boost}(Z+jet)$
- $1/\sigma_{Z/\gamma^*} \times d\sigma_{Z/\gamma^*+jet}/d\Delta\phi_{Z,jet}$

all for two sets of kinematic cuts: $p_T^{jet} > 20$ GeV with $p_T^Z > 25$ GeV; and $p_T^{jet} > 20$ GeV with $p_T^Z > 45$ GeV, where:

- The Z/γ^* is selected from a pair of opposite charge muons, with $|y^\mu| < 1.7$ and $65 < M_{\mu,\mu} < 115$ GeV.
- Jets are constructed the D0 Run-II seeded mid-point cone algorithm with a cone size of 0.5, and a split/merge fraction of 0.5. Jets are required to have $|y^{jet}| < 2.8$, then the highest p_T jet is selected and required to have $p_T > 20$ GeV.

Predictions from pQCD are obtained using the $Z/\gamma^* + 1$ parton NLO calculation in MCFM v5.3, together with the CTEQ6.6M PDF [27]. This produces a NLO distribution for $\Delta y_{Z,jet}$ and $y_{boost}(Z+jet)$, but only the LO corrections to $\Delta\phi_{Z,jet}$ (excluding the bin at π , which contains the higher order terms). Re-normalization and factorization scales are set to the sum in quadrature of the mass and p_T of the Z/γ^* in each event, and uncertainties are derived by varying the scale up and down by a factor of two, both for the differential distribution and the inclusive Z/γ^* cross section used in normalisation. PDF uncertainties are assessed using the CTEQ6.6M error sets, again taking into account the effect on the differential distribution and the inclusive Z/γ^* cross section used in normalisation. MCFM provides a parton level prediction, so corrections to the particle level must be applied. Such non-perturbative corrections for hadronisation and the underlying event have been derived from a sample of $Z+jet$ events generated with PYTHIA v6.419 using the leading order CTEQ5L PDF [28] with tune DW [29]. These are derived by comparing the full prediction (taken from the final state particles, including the underlying event) to the purely perturbative part (calculated from partons taken after the parton shower, with no underlying event). These corrections are typically around 4%. The low $\Delta\phi_{Z,jet}$ (< 1.5 rad) region is dominated by non-perturbative effects, so the pQCD calculation for this bin is not shown. Corrections for QED FSR from the muons are also derived from the same PYTHIA sample, by comparing the prediction calculated using the muons after FSR to those taking the generated boson; these are typically less than 1% after accounting for the effect on the inclusive Z/γ^* cross section, and are the result primarily of events migrating out of the mass window.

Comparisons are also made to three event generators. Current ALPGEN versions are not compatible with the CTEQ6.6M PDF, so in order to use a consistent PDF set with all three, CTEQ6.1M [30] is chosen. A sample of events is generated with ALPGEN v2.13 with up to three partons in the matrix element calculation, and the factorization and re-normalization scales set to the sum in quadrature of the mass and p_T of the Z . Jets from the matrix element calculation are required to have $p_T > 13$ GeV, and $\Delta R(jet, jet) > 0.4$. These events are hadronised using both PYTHIA v6.325 (with tune QW), and HERWIG (using JIMMY for multiple parton interactions), resulting in two predictions. A sample of events is also generated with SHERPA v1.1.1, again with up to three partons in the matrix element calculation, and requiring jets from the matrix element calculation to have $p_T > 15$ GeV, and $\Delta R(jet, jet) > 0.4$. Finally, an inclusive $Z/\gamma^* \rightarrow \mu^+\mu^-$ sample is generated with PYTHIA v6.419, with underlying event tune QW [29] and the 2-loop prescription for α_s . In defining the observables in simulation, some care must be taken to avoid dependence on the model of the underlying event or QED final state radiation. In all cases, the Z/γ^* is reconstructed from the highest p_T opposite charge stable muons, and all other final state stable particles are passed to the jet reconstruction algorithm, but excluding any photons in a 0.2 cone around each muon (to remove any QED FSR off these muons).

The normalised differential cross sections are shown binned in $\Delta\phi_{Z,jet}$ (Fig. 1), $\Delta y_{Z,jet}$ (Fig. 2) and $y_{boost}(Z+jet)$ (Fig. 3). The data points are placed at the bin center, defined as the point where the differential cross section in simulation (re-weighted to match the shape in data) is equal to the bin value [31]. The data are shown with statistical uncertainties (inner error bar), and combined statistical and systematic uncertainties (outer error bar). Each theoretical curve is normalised to the total Z/γ^* production cross section predicted by that theory. For clarity, only the predictions of NLO pQCD and ALPGEN are shown in the upper portion of each figure, though the prediction from NLO pQCD + corrections is not shown at low $\Delta\phi_{Z,jet}$, where the non-perturbative effects dominate. In the lower portion of each figure, the distributions are divided by the prediction from ALPGEN with PYTHIA showering. The NLO pQCD prediction is also shown with the combined scale and PDF uncertainties as a hatched region; the scale uncertainty is a factor of two or more larger than the PDF uncertainty in all regions.

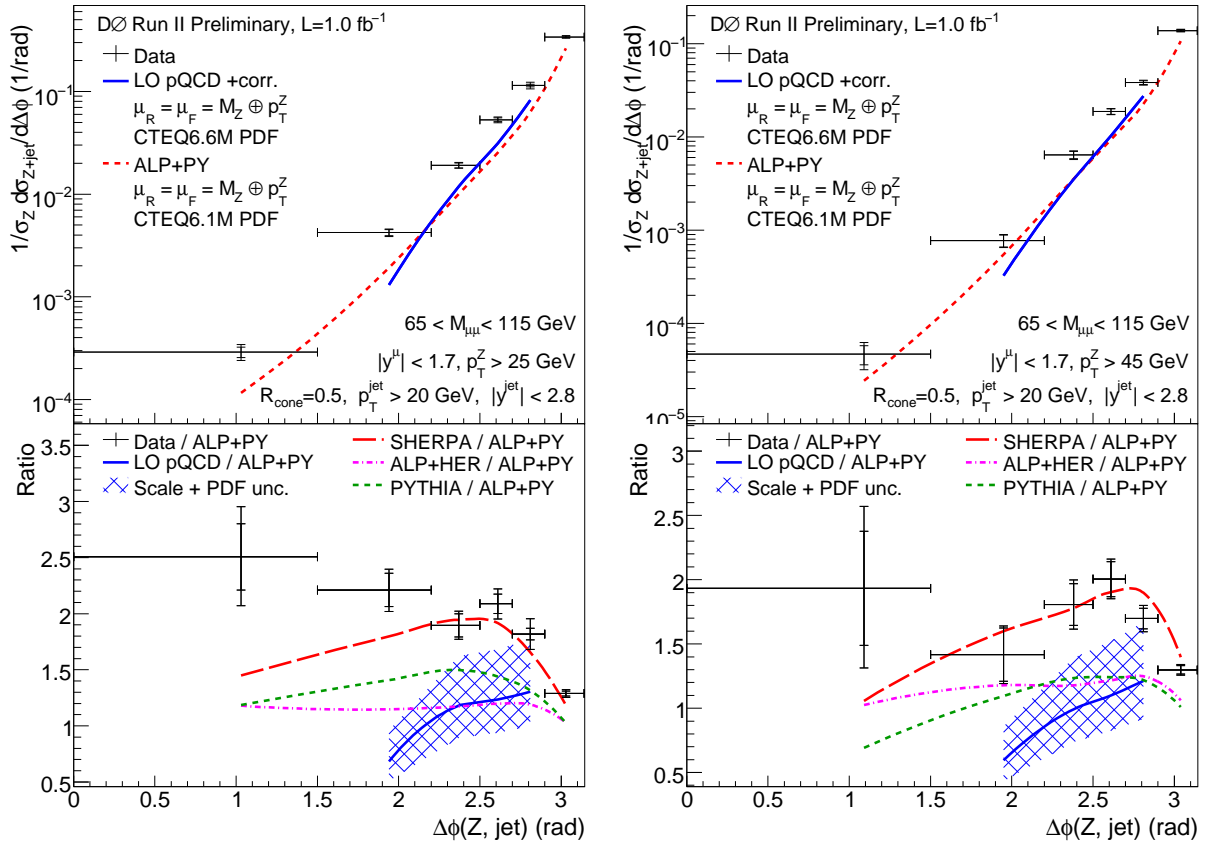


FIG. 1: The measured cross section in bins of $\Delta\phi_{Z,jet}$ for $Z/\gamma^* + jet + X$ events (upper), and the ratio of data and predictions from NLO pQCD, SHERPA and PYTHIA to the prediction from ALPGEN (lower). Left: for $p_T^Z > 25$ GeV; right: for $p_T^Z > 45$ GeV.

V. CONCLUSIONS

In summary, we have presented the first measurements at a hadron collider of the $Z/\gamma^* + jet + X$ cross section differential in $\Delta\phi_{Z,jet}$, $\Delta y_{Z,jet}$, and $y_{boost}(Z + jet)$. The measurements were made using a sample corresponding to $0.97 \pm 0.06 \text{ fb}^{-1}$ of integrated luminosity recorded by the D0 experiment in $p\bar{p}$ collisions at $\sqrt{s} = 1.96$ TeV.

The NLO pQCD calculation provides a good description of the data; an overall normalisation difference is observed, but is within the combined data and theory uncertainties. The LO $\Delta\phi_{Z,jet}$ prediction does not describe the data, and a NLO calculation is not yet available. Of the event generators, SHERPA generally provides the best description of both the shape and normalisation of the data. However, in the sample with $p_T^Z > 45$ GeV, SHERPA does not provide a good description of $\Delta y_{Z,jet}$ or $y_{boost}(Z + jet)$. The predictions from ALPGEN seem to be the opposite, providing a good description of the only the shape of $\Delta y_{Z,jet}$ and $y_{boost}(Z + jet)$ for $p_T^Z > 45$ GeV. The predictions from PYTHIA show significant normalisation differences, though a reasonable description of the shape of some of the distributions.

These measurement tests the current best predictions for heavy boson + jet production at hadron colliders. They are also essential inputs for the tuning of event generators, and the modeling of $V + jet$ production at hadron colliders. Improving the modeling of the important signal will lead to increased sensitivity to rare and new physics.

We thank John Campbell for useful discussions and input on MCFM. We thank the staffs at Fermilab and collaborating institutions, and acknowledge support from the DOE and NSF (USA); CEA and CNRS/IN2P3 (France); FASI, Rosatom and RFBR (Russia); CNPq, FAPERJ, FAPESP and FUNDUNESP (Brazil); DAE and DST (India); Colciencias (Colombia); CONACyT (Mexico); KRF and KOSEF (Korea); CONICET and UBACyT (Argentina); FOM (The Netherlands); STFC (United Kingdom); MSMT and GACR (Czech Republic); CRC Program, CFI, NSERC and WestGrid Project (Canada); BMBF and DFG (Germany); SFI (Ireland); The Swedish Research Council (Sweden);

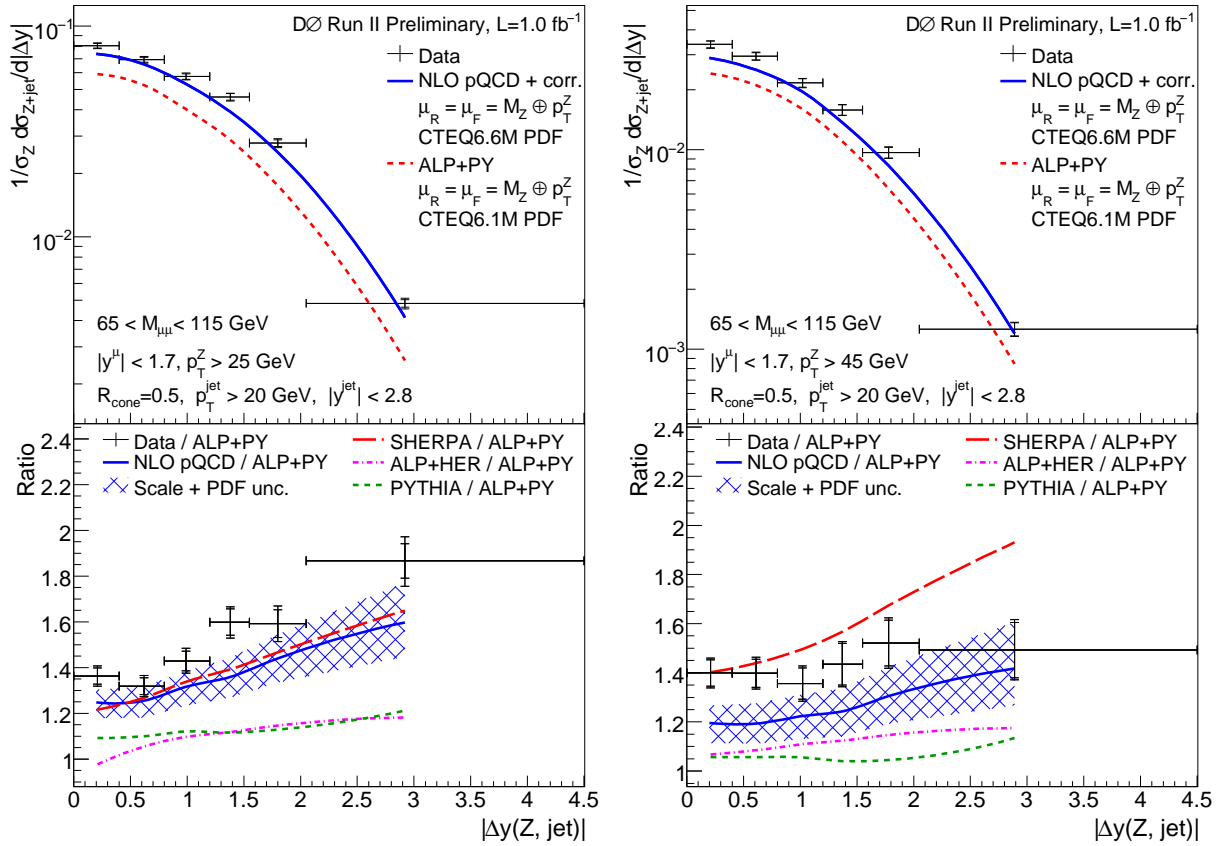


FIG. 2: The measured cross section in bins of $\Delta y_{Z,\text{jet}}$ for $Z/\gamma^* + \text{jet} + X$ events (upper), and the ratio of data and predictions from NLO pQCD, SHERPA and PYTHIA to the prediction from ALPGEN (lower). Left: for $p_T^Z > 25$ GeV; right: for $p_T^Z > 45$ GeV.

CAS and CNSF (China); and the Alexander von Humboldt Foundation (Germany).

-
- [1] CDF Collaboration, T. Affolder *et al.*, Phys. Rev. Lett. **84**, 845 (2000).
[2] D0 Collaboration, V. M. Abazov *et al.*, Phys. Rev. Lett. **100**, 102002 (2008).
[3] D0 Collaboration, V. M. Abazov *et al.*, Phys. Rev. D **76**, 012003 (2007).
[4] D0 Collaboration, V. M. Abazov *et al.*, Phys. Lett. B **658**, 112 (2008).
[5] D0 Collaboration, V. M. Abazov *et al.*, Phys. Lett. B **658**, 112 (2008).
[6] CDF Collaboration, T. Aaltonen *et al.*, Phys. Rev. Lett. **100**, 102001 (2008).
[7] D0 Collaboration, V. M. Abazov *et al.*, arXiv:0903.1748 [hep-ex] (2009), submitted to Phys. Lett. B.
[8] D0 Collaboration, V. M. Abazov *et al.*, Phys. Rev. Lett. **94**, 161801 (2005).
[9] CDF Collaboration, T. Aaltonen *et al.*, Phys. Rev. D **74**, 032008 (2006).
[10] D0 Collaboration, V. M. Abazov *et al.*, Phys. Lett. B **666**, 23 (2008).
[11] CDF Collaboration, T. Aaltonen *et al.*, Phys. Rev. Lett. **100**, 091803 (2008).
[12] T. Andeen *et al.*, FERMILAB-TM-2365 (2007).
[13] J. Campbell and R. K. Ellis, Phys. Rev. D **65**, 113007 (2002).
[14] T. Sjöstrand *et al.*, Comput. Phys. Commun. **135**, 238 (2001).
[15] G. Corcella *et al.*, JHEP **0101**, 010 (2001).
[16] T. Gleisberg *et al.*, JHEP **0402**, 056 (2004).
[17] M. L. Mangano *et al.*, JHEP **0307**, 001 (2003).
[18] S. Hoeche *et al.*, arXiv:hep-ph/0602031 (2006).
[19] D0 Collaboration, V. M. Abazov *et al.*, Nucl. Instrum. Methods Phys. Res. A **565**, 463 (2006).
[20] $\eta = -\ln[\tan(\theta/2)]$, where θ is the polar angle, defined with respect to the proton beam axis.
[21] G. C. Blazey *et al.*, in *Proceedings of the Workshop: QCD and Weak Boson Physics in Run II*, edited by U. Baur, R. K. Ellis, and D. Zeppenfeld, Fermilab-Pub-00/297 (2000).

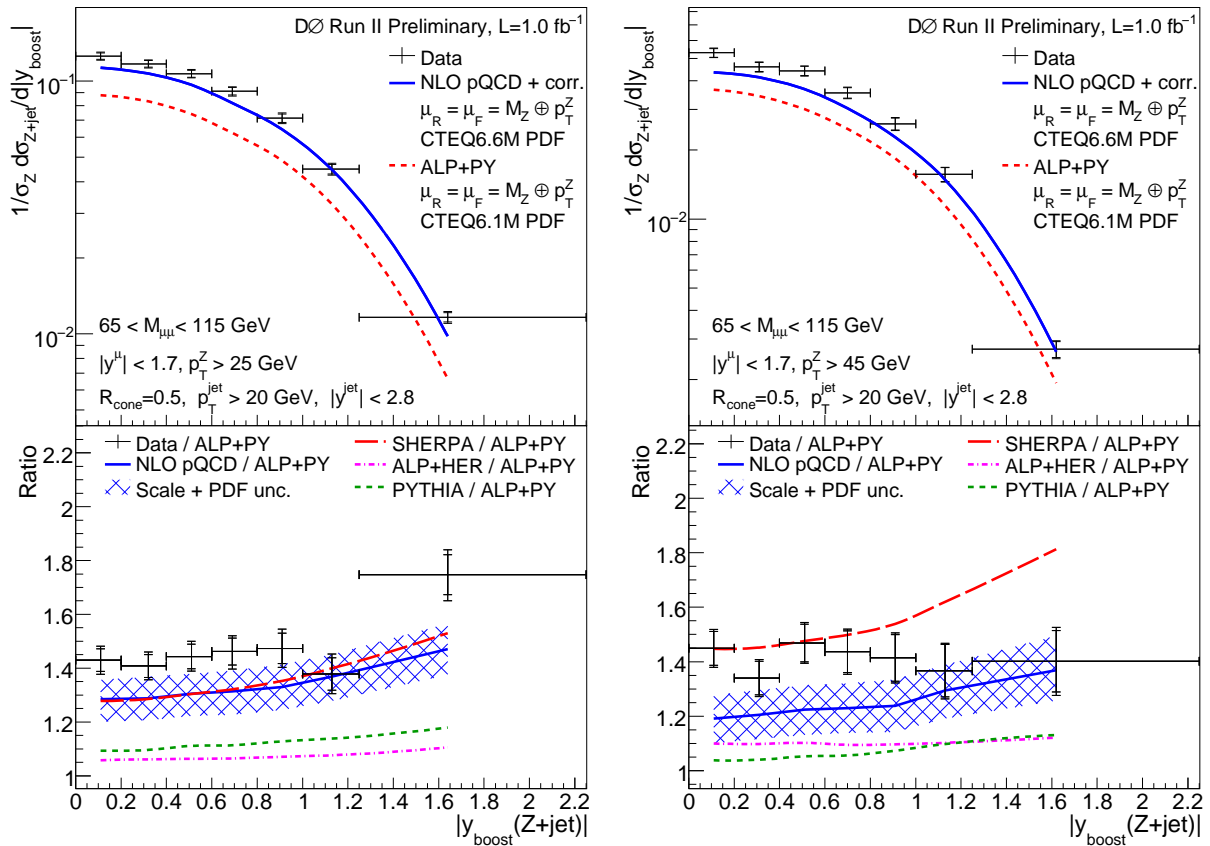


FIG. 3: The measured cross section in bins of $y_{boost}(Z + \text{jet})$ for $Z/\gamma^* + \text{jet} + X$ events (upper), and the ratio of data and predictions from NLO pQCD, SHERPA and PYTHIA to the prediction from ALPGEN (lower). Left: for $p_T^Z > 25$ GeV; right: for $p_T^Z > 45$ GeV.

- [22] Rapidity is defined as $y = \ln \frac{E-p_z}{E+p_z}$, where E is the energy, and p_z the component of momentum parallel to the proton beam direction. ϕ is the azimuthal angle.
- [23] C. Buttar *et al.*, arXiv:hep-ph/0803.0678 (2008). A detailed discussion is given in Sect. 9.
- [24] J. Pumplin *et al.*, JHEP **0207** 012 (2002).
- [25] CDF Collaboration, T. Affolder *et al.*, Phys. Rev. D **65**, 092002 (2002).
- [26] R. Brun and F. Carminati, in *CERN Program Library Long Writeup W5013*, 1993 (unpublished).
- [27] P. M. Nadolsky *et al.*, Phys.Rev.D **78** 013004 (2008).
- [28] H. L. Lai *et al.*, Eur. Phys. J. C **12**, 375 (2000).
- [29] M. G. Albrow *et al.*, arXiv:hep-ph/0610012 (2006).
- [30] D. Stump *et al.*, JHEP **0310**, 046 (2003).
- [31] G. D. Lafferty and T. R. Wyatt, Nucl. Instrum. Methods Phys. Res. A **355**, 541 (1995).